Random magnetocrystalline anisotropy in two-phase nanocrystalline systems

K. Suzuki* and J. M. Cadogan
School of Physics, The University of New South Wales, Sydney 2052, Australia
(Received 22 December 1997)

In order to clarify the effect of the exchange stiffness in the intergranular phase on the exchange correlation length (L_{ex}) and the random magnetocrystalline anisotropy ($\langle K_1 \rangle$) of two-phase nanocrystalline soft magnetic materials, the hyperfine fields (^{57}Fe), coercivity and remanence to saturation ratio of nanocrystalline $Fe_{91}Zr_7B_2$ have been studied in the temperature range from 77 to 473 K. We observe that the coercivity of the nanocrystalline $Fe_{91}Zr_7B_2$ in the temperature range near the Curie temperature of the intergranular amorphous phase (T_C^{am}) varies as approximately the -6th power of the mean hyperfine field of the intergranular phase. This indicates that L_{ex} near $T \sim T_C^{am}$ is mostly governed by the exchange stiffness of the intergranular amorphous phase and $\langle K_1 \rangle$ of the Fe-Zr-B sample should vary as the -3rd power of the exchange stiffness constant in the intergranular region. These results are explained well by our extended two-phase random anisotropy model in which two local exchange stiffness constants are considered for the spin-spin correlation within L_{ex}. [S0163-1829(98)03629-7]

I. INTRODUCTION

Excellent magnetic softness has been observed in various amorphous[1] or nanocrystalline[2] systems. The origin of the magnetic softness in these materials is due to the important condition that the structural correlation length (atomic distance in the case of amorphous materials or grain size in nanocrystalline systems) is shorter than the exchange correlation length (L_{ex}) over which spins are coupled via the exchange interaction. Alben, Becker, and Chi[3] have described the effective anisotropy energy of the amorphous materials based on a statistical argument, the so-called random anisotropy model. The effective anisotropy energy density in this model is given by the square root of the mean-square fluctuation of the anisotropy energy in the exchange coupled volume ($\sim L_{ex}^3$). Herzer[4,5] has shown that the random anisotropy model explains the effective anisotropy energy even in nanocrystalline systems and predicted that the coercivity H_c varies as the sixth power of the grain size (D) in the range $D < L_{ex}$.

Since Herzer's first application of the random anisotropy model to nanocrystalline Fe-Si-B-Nb-Cu,[4] this model has been employed widely to explain the origin of the magnetic softness in various nanocrystalline systems.[6,7] Most of the nanocrystalline soft magnetic alloys reported so far were prepared by primary crystallization of amorphous precursors and thus the resultant microstructure contains a considerable amount of the residual amorphous phase.[8] However, the original random anisotropy model only deals with single-phase systems and hence the model is not strictly applicable to the variety of unique magnetic behaviors which originate from the two-phase nature itself. These unique behaviors include (i) the magnetic hardening at elevated temperatures near the Curie temperature of the intergranular amorphous phase[4] at which the intergranular exchange coupling is reduced dramatically and (ii) the magnetic hardening at the initial stage of the nanostructural evolution[9] where the volume fraction of the residual amorphous phase is substantial. Hernando *et al.*[10] have recently proposed an extended model in which the decay of the exchange interaction within the intergranular amorphous region as well as the volume fraction of the amorphous phase is considered. Their extended model can explain the latter problem but, as the authors discussed in their paper, this model failed to describe the magnetic hardening with increasing temperature towards T_C^{am}. We are particularly interested in this unresolved problem since the answer to this problem would establish a physical basis for the magnetic softness in the two-phase nanocrystalline soft magnetic materials.

In actual nanocrystalline samples, the contributions of the induced anisotropies (e.g., magnetoelastic or annealing-induced anisotropies) to the magnetization process always complicate the treatment of the intrinsic physical problems. In this report, we first consider the applicability of the random anisotropy model and we select an appropriate nanocrystalline sample in which the effect of the induced anisotropies is negligible relative to $\langle K_1 \rangle$. The temperature dependences of the various magnetic properties for the selected nanocrystalline sample are then examined. We have employed ^{57}Fe Mössbauer spectroscopy to investigate the temperature dependence of the magnetization since this method provides intrinsic magnetic properties without the need to apply an external magnetic field and also measures the magnetic properties of the residual amorphous phase and the nanocrystallites separately. Finally, the observed temperature dependence of magnetic properties including coercivity and the mean hyperfine field of the residual amorphous phase are discussed, based on a new extended random anisotropy model where the effects of the volume fraction and the exchange stiffness of the residual amorphous phase are considered.

II. APPLICABILITY OF THE RANDOM ANISOTROPY MODEL IN ACTUAL NANOCRYSTALLINE SYSTEMS

In Herzer's model[4,5] the reduction of the effects of the intrinsic magnetocrystalline anisotropy constant (K_1) is

based on the following random-walk consideration:

$$\langle K_1\rangle = \frac{K_1}{\sqrt{N}}, \tag{1}$$

where $\langle K_1\rangle$ is the random magnetocrystalline anisotropy (i.e., the fluctuating part of the magnetocrystalline anisotropy energy) which governs the magnetization process in the sample. N is the number of grains in a magnetically coupled volume which, in bulk-form systems, is

$$N = \left(\frac{L_{\rm ex}}{D}\right)^3, \tag{2}$$

where the exchange correlation length $L_{\rm ex}$ is determined by the competition between the anisotropy and exchange energy terms and is defined as

$$L_{\rm ex} = \varphi\sqrt{\frac{A}{\langle K\rangle}}. \tag{3}$$

Here, A is the exchange stiffness constant and φ is a parameter which reflects both the symmetry of the effective anisotropy constant $\langle K\rangle$ and the total spin rotation angle over the exchange-correlated coupling chain. Provided that the random magnetocrystalline anisotropy is the dominant anisotropy in the system and the effective anisotropy constant is approximated by $\langle K\rangle$ (i.e., $\langle K\rangle \approx \langle K_1\rangle$), the effective length of $L_{\rm ex}$ can then be determined self-consistently using Eqs. (1)–(3), yielding

$$L_{\rm ex} \approx \varphi^4 \frac{A^2}{K_1^2 D^3}, \tag{4}$$

which leads to the well-known relation

$$\langle K\rangle \approx \frac{1}{\varphi^6}\frac{K_1^4 D^6}{A^3}. \tag{5}$$

In this argument, Herzer assumed $\varphi = 1$ rad ($\varphi = \sqrt{4/3}$ in the model of Alben *et al.*[3]). The origin of these φ values was not discussed in detail in their models and hence the absolute value of $\langle K\rangle$ is not free from uncertainty. However, the significance of Herzer's approach lies in the derived power laws: D^6, K_1^4, and A^{-3}. The above scalinglike argument is valid under the condition $\langle K\rangle \approx \langle K_1\rangle$.

Naturally, the effective anisotropy in the nanocrystalline materials may have contributions from induced anisotropies other than the random magnetocrystalline anisotropy and hence the effective anisotropy constant in actual systems is more correctly

$$\langle K\rangle = \sqrt{\langle K_1\rangle^2 + \sum_i K_{ui}^2}, \tag{6}$$

where K_u is the induced uniaxial anisotropy. This term comprises at least the contribution from the following magnetoelastic anisotropy:

$$K_u^{\rm el} = \frac{3}{2}|\lambda_s \sigma|, \tag{7}$$

where λ_s is the saturation magnetostriction and σ is the residual stress. Consequently, if the K_u term in Eq. (6) is significant relative to $\langle K_1\rangle$ (e.g., samples with large magnetostriction and small grain sizes), the $\langle K\rangle$ value is governed by K_u. In such a case, one may no longer see the effect of grain refinement on the coercivity variation. More importantly, the critical condition $\langle K\rangle \approx \langle K_1\rangle$ obviously does not hold and hence the contribution of K_u to $\langle K\rangle$ alters the renormalization process of $L_{\rm ex}$ and both Eqs. (4) and (5) change. Therefore, an exact application of the D^6, K_1^4, and A^{-3} scalinglike rules should be strictly limited to those samples whose magnetization process is governed by the random magnetocrystalline anisotropy $\langle K_1\rangle$.

Another possible source of discrepancy between the model and experiments is the fact that the model discussed above assumes single-phase materials, while the nanocrystalline soft magnetic materials are two-phase systems. The extension of the random anisotropy model to two-phase systems has recently been reported by Herzer[11] and Hernando *et al.*[10] In Herzer's extended approach, quadratic contributions of the random local anisotropies from different phases to the mean-square amplitude of the anisotropy energy were considered and $\langle K\rangle$ in his extended approach for $\varphi = 1$ has been given by

$$\langle K\rangle \approx \left(\sum_i \frac{\nu_i D_i^3 K_i^2}{A^{3/2}}\right)^2, \tag{8}$$

where ν_i and K_i are the volume fraction and the local magnetocrystalline anisotropy constant of the ith phase, respectively. Provided that the effective local anisotropy constant of the residual amorphous phase in the two-phase nanocrystalline materials is negligibly small relative to K_1 of the bcc-Fe nanocrystallites, Eq. (8) is approximated by

$$\langle K\rangle \approx (1 - V_{\rm am})^2 \frac{K_1^4 D^6}{A^3}, \tag{9}$$

where $V_{\rm am}$ is the volume fraction of the residual amorphous phase. It should be noted that the original D^6, K_1^4, and A^{-3} laws are maintained in this two-phase model at a constant $V_{\rm am}$ value. The assumption in this model that the local anisotropy in the residual amorphous phase is negligibly smaller than K_1 can be tested by checking whether the sample magnetization process reflects the cubic symmetry of $\langle K_1\rangle$ or not. If the local anisotropy constant of the amorphous part is significant relative to $\langle K_1\rangle$ then $\langle K\rangle$ reflects uniaxial anisotropy symmetry. Therefore, in any case where Fe-based nanocrystalline soft magnetic alloys reveal the cubic anisotropy symmetry of $\langle K_1\rangle$, the above scalinglike argument which predicts the D^6, K_1^4, and A^{-3} laws should be applicable. We have considered this important criterion for the applicability of the nanocrystalline random anisotropy model throughout the present report.

III. EXPERIMENTAL PROCEDURES

Amorphous $Fe_{91}Zr_7B_2$ was prepared in an argon atmosphere by a single roller melt spinner. The amorphous samples were sealed in evacuated quartz tubes (10^{-3} Pa) and annealed for periods of 60 s to 1080 ks at temperature of

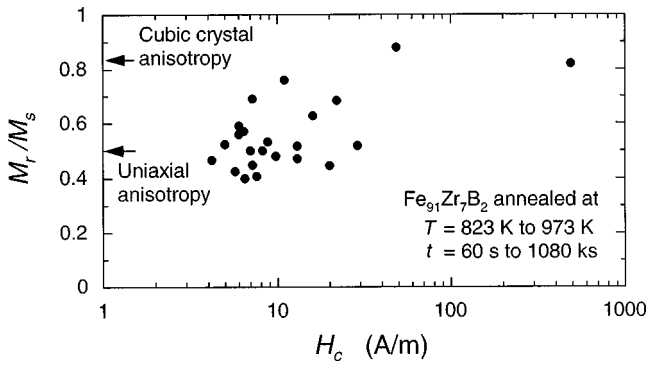

FIG. 1. Relation between coercivity (H_c) and the remanence to saturation ratio (M_r/M_s) for nanocrystalline $Fe_{91}Zr_7B_2$.

823 to 973 K using a salt bath. ^{57}Fe Mössbauer spectroscopy was carried out using a conventional constant-acceleration spectrometer and a ^{57}Co Rh source. The Mössbauer spectra were fitted using a histogram method.[12] The coercivity was measured using a dc B-H loop tracer in the temperature range from 77 to 480 K at a heating rate of 2 K/min. The volume fraction of the residual amorphous phase ($V_{\rm am}$) and the mean grain size (D) were evaluated from ^{57}Fe Mössbauer results and the peak width of the $(110)_{\rm bcc}$ x-ray reflection, respectively. The evaluation of $V_{\rm am}$ was made by assuming (i) the same recoil-free fractions for the bcc and amorphous phases and (ii) the Fe content of the nanocrystallites is 98 at. %, which has been estimated using atom-probe field-ion microscopy.[8]

IV. RESULTS

A. Anisotropy symmetry

As discussed in Sec. II the application of the random anisotropy model to actual nanocrystalline materials should be limited to the case where $\langle K_1\rangle$ is relevant to the magnetization process. In order to select an ideal nanocrystalline $Fe_{91}Zr_7B_2$ sample to which the random anisotropy model is applicable, the remanence to saturation ratio (M_r/M_s) of the $Fe_{91}Zr_7B_2$ samples annealed under various conditions was examined. Figure 1 shows the relation between M_r/M_s and coercivity for the nanocrystalline $Fe_{91}Zr_7B_2$ samples annealed in the temperature range from 823 to 973 K for periods from 60 s to 1080 ks. In this figure, the theoretical remanence ratio predicted in the Stoner-Wohlfarth model for randomly oriented noninteracting particles with uniaxial (0.5) and cubic (0.83) crystalline symmetry[13] are marked. It has been shown by Chikazumi[14] that these theoretical M_r/M_s values can also be retained for magnetization processes proceeding by domain-wall movement. The remanence ratio in Fig. 1 tends to decrease with decreasing H_c towards the value of uniaxial symmetry and M_r/M_s near the value of cubic symmetry is limited to two samples with relatively high coercivity values. This shows that the magnetization process in the low-H_c region is mostly governed by induced anisotropies, indicating that the K_u term in Eq. (6) is greater than $\langle K_1\rangle$. On the contrary, the high M_r/M_s values near 0.83 associated with high H_c indicate that the absolute values of $\langle K_1\rangle$ in these two samples are large, relative to K_u, and thus $\langle K_1\rangle$ indeed governs the magnetization process. These two particular samples were prepared by annealing amorphous $Fe_{91}Zr_7B_2$ at 823 K for 60 s and 973 K for 3.6 ks, respectively.

It has previously been reported[15] that the amorphous $Fe_{91}Zr_7B_2$ alloy annealed at 973 K for 3.6 ks contains cubic Fe_3Zr. We have confirmed the formation of Fe_3Zr in our sample annealed at 973 K for 3.6 ks by x-ray diffractometry. The high-H_c value (490 A/m) associated with the cubic anisotropy symmetry of this sample is most likely due to the large K_1 of the cubic Fe_3Zr phase and hence $\langle K\rangle$ of this sample does not reflect the random magnetocrystalline anisotropy of the bcc-Fe phase. Consequently, we will focus our attention on the $Fe_{91}Zr_7B_2$ sample annealed at 823 K for 60 s whose microstructure is composed only of the nanocrystalline bcc and the residual amorphous phase. The mean grain size of this sample was evaluated to be 12.6 nm.

B. Temperature dependence of magnetic properties

Among the magnetic and structural parameters relevant to $\langle K\rangle$ in the two-phase random anisotropy model, D and $V_{\rm am}$ are temperature independent in the range well below the crystallization temperature whereas A and K_1 depend on temperature. Consequently, the thermomagnetic measurements provide us with an ideal experimental opportunity within which the effect of A or K_1 on the random magnetocrystalline anisotropy can be discussed quantitatively.

The temperature dependence of the ^{57}Fe hyperfine field in the nanocrystalline $Fe_{91}Zr_7B_2$ sample was examined by means of ^{57}Fe Mössbauer spectroscopy. Amorphous $Fe_{91}Zr_7B_2$ in the rapidly quenched state was also examined for comparison. Figure 2 shows the ^{57}Fe Mössbauer spectra and corresponding hyperfine-field distributions, $P(B_{\rm hf})$, of the amorphous $Fe_{91}Zr_7B_2$ alloy in the temperature range from 80 to 220 K. A broad distribution of hyperfine-field typical of amorphous ferromagnetic systems is seen and the mean hyperfine-field ($\langle B_{\rm hf}\rangle$) decreases with increasing temperature.

The temperature dependence of the Mössbauer spectra for the nanocrystalline $Fe_{91}Zr_7B_2$ alloy is shown in Fig. 3. Three subspectral components; a broad subspectrum for the residual amorphous phase and two sextets for the bcc-Fe nanocrystallites, are necessary to fit the spectra satisfactorily. The relative area of the amorphous subspectrum ($R_{\rm am}$) was estimated to be 0.48 by fitting the spectrum at 295 K where the overlap between the various subspectral components is less pronounced. A constant $R_{\rm am}$ value of 0.48 ± 0.01 was then chosen for the subsequent fitting of the spectra at other temperatures in order to avoid any error in $\langle B_{\rm hf}\rangle$ due to the fluctuation of $R_{\rm am}$. In addition, the same line intensity ratio was used for all the subspectral components at each temperature since the magnetization in both the bcc and amorphous phases in the sample is expected to be coupled via the exchange interaction. The area ratio of the two sextets from the bcc phase is about 95:5 and $B_{\rm hf}$ of the minor sextet is smaller than that of the major sextet by about 10% [$B_{\rm hf}$(major) $=33$ T at 295 K]. The smaller $B_{\rm hf}$ value of the minor sextet represents those Fe atoms having some nonmagnetic near-neighbor atoms in the bcc lattice, consistent with the previous atom-probe field-ion microscopy study[8] which clearly

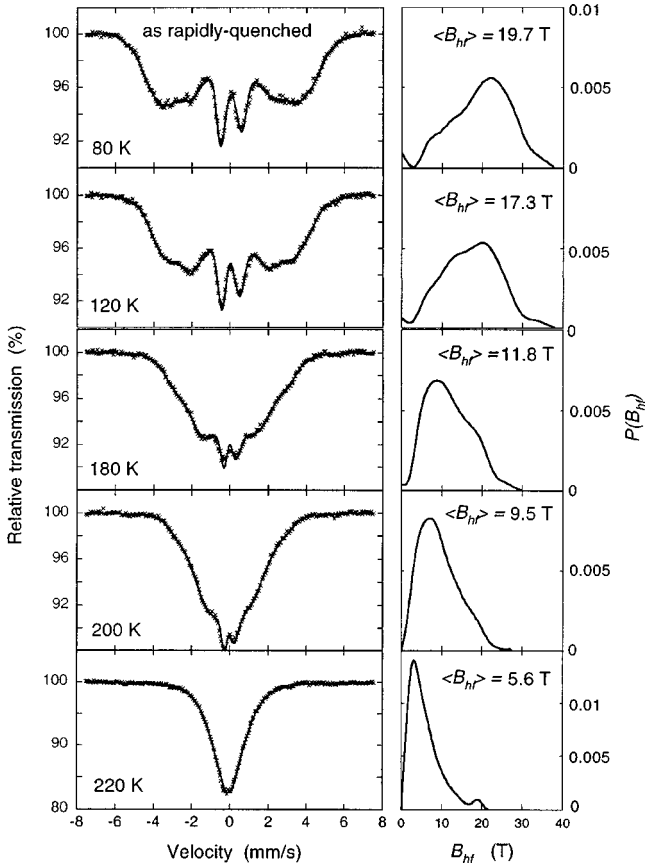

FIG. 2. Mössbauer spectra and hyperfine-field distributions at various temperatures for $Fe_{91}Zr_7B_2$ in a rapidly quenched state.

indicates the dissolution of solute elements in the bcc nanocrystallites in an $Fe_{90}Zr_7B_3$ sample.

We have analyzed the temperature dependence of $\langle B_{\rm hf}\rangle$ in both the amorphous and nanocrystalline $Fe_{91}Zr_7B_2$ samples in order to estimate the Curie temperature. Handrich[16] described the temperature dependence of the spontaneous magnetization (M_s) in amorphous systems by taking into account the distribution of the exchange integral in the molecular-field approximation:

$$M_s(T)=\frac{1}{2}M_s(0)\{B_S[x(1+\Delta)]+B_S[x(1-\Delta)]\}, \tag{10}$$

where $B_s(x)$ is the Brillouin function and Δ is a parameter representing the exchange distribution. The temperature dependence of $\langle B_{\rm hf}\rangle$ derived from our Mössbauer results is analyzed based on this model. Figure 4 shows the relationship between the reduced mean hyperfine field and the reduced temperature for the amorphous and nanocrystalline $Fe_{91}Zr_7B_2$ alloys together with the theoretical curves with $B_{1/2}$ (the Brillouin function for $S=1/2$). As we see in this figure, the $\langle B_{\rm hf}(T)\rangle$ of both the amorphous and nanocrystalline samples are well fitted by the Handrich model. The T_C, $\langle B_{\rm hf}(0)\rangle$, and Δ values for these theoretical curves were determined by least-squares fitting. The Curie temperatures of the amorphous phase in these samples were also estimated from the temperature dependence of the γ-ray absorption at zero velocity, the so-called Mössbauer thermal scan method (Fig. 5). Table I summarizes these fitting parameters together with the Curie temperatures estimates. Our estimated Curie temperature of the rapidly quenched $Fe_{91}Zr_7B_2$ sample ($\sim$230 K) agrees well with the value (230 ± 5 K) estimated by Barandiarán *et al.*[17] for an amorphous phase of the same alloy composition. Although the T_C values of the residual amorphous phase in the table contain relatively large errors (370 ± 10 K), this value is clearly higher than the value in the rapidly quenched state. This increase in the Curie temperature of the amorphous matrix phase upon crystallization is one of the most important effects in the nanocrystalline Fe-M-B (M=Zr, Hf, and Nb) soft magnetic alloys[18] because the exchange coupling between nanocrystallites is strengthened by the increase in the Curie temperature of the intergranular region and hence the magnetically coupled volume ($L_{\rm ex}^3$) increases. Hernando, Navarro, and Gorria[19] reported that the Curie temperature of the intergranular amorphous phase can be enhanced by $\sim$100 K due to the Fe-exchange field penetrating from the bcc-Fe nanocrystallites. This exchange penetration effect together with the enrichment of the solute elements in the residual amorphous phase due to the chemical redistribution upon primary crystallization can explain the observed increase in the Curie temperature.

The hyperfine-field distributions of the amorphous phase in Figs. 2 and 3 show complex structures. Similar results were reported for some Fe-rich amorphous Fe-Zr alloys[20,21] and the complex $P(B_{\rm hf})$ distribution has been attributed by some authors to the formation of magnetic clusters. On the other hand, the complex shape of the $P(B_{\rm hf})$ distribution for the residual intergranular amorphous phase is a common problem in nanocrystalline soft magnetic systems[22,23] which was considered to be due to the structural and chemical inhomogeneity in the intergranular region. We note, though, that some authors have pointed out that the $P(B_{\rm hf})$ distribution of amorphous systems can be bimodal simply as a mathematical artifact[24,25] and thus, one cannot unequivocally conclude cluster formation or inhomogeneity purely on the basis of the bimodal $P(B_{\rm hf})$ distributions. Thus, there is the possibility, suggested by our results, that the residual amorphous phase in our nanocrystalline sample could conceivably be magnetically inhomogeneous. However, as demonstrated in Figs. 4 and 5, the temperature dependence of $\langle B_{\rm hf}\rangle$ for the residual amorphous phase is extremely well described by the molecular field approximation with a single critical point, indicating that the spins in the residual amorphous phase behave cooperatively despite any possible magnetic inhomogeneity. Consequently, the temperature dependence of intrinsic magnetic properties such as the spontaneous magnetization and the exchange stiffness constant of the residual intergranular amorphous phase in our $Fe_{91}Zr_7B_2$ sample appear to behave as conventional ferromagnetic amorphous systems.

The temperature dependence of the coercivity and the remanence ratio for the nanocrystalline $Fe_{91}Zr_7B_2$ sample annealed at 823 K for 60 s is shown in Fig. 6. H_c of the nanocrystalline $Fe_{91}Zr_7B_2$ sample increases slowly with temperature from 5.7 A/m at 77 K to 56 A/m at room temperature and then begins to increase significantly near $T_C^{\rm am}$ where the intergranular magnetic coupling deteriorates as a result of the ferromagnetic to paramagnetic transition of the intergranular amorphous phase. We have confirmed that H_c is

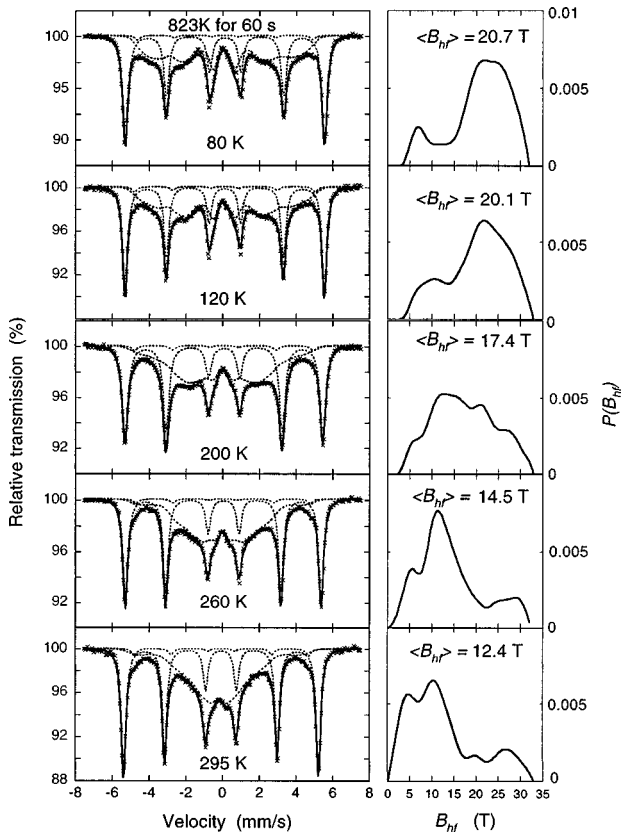

FIG. 3. Mössbauer spectra and hyperfine-field distributions at various temperatures for $Fe_{91}Zr_7B_2$ annealed at 823 K for 60 s.

completely reversible in the entire temperature range shown in Fig. 6 and hence any effect of the annealing upon the measurement can be neglected. This phenomenon was discovered by Herzer[4] and is known as a typical feature of the two-phase nanocrystalline soft magnetic materials with two distinct Curie temperatures. M_r/M_s in Fig. 6 shows a tendency to decrease with decreasing temperature and the value

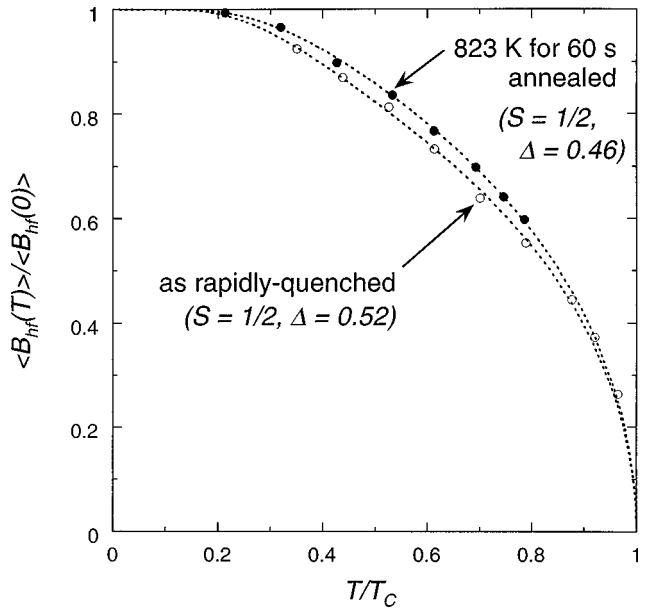

FIG. 4. Relation between the reduced mean hyperfine-field and the reduced temperature.

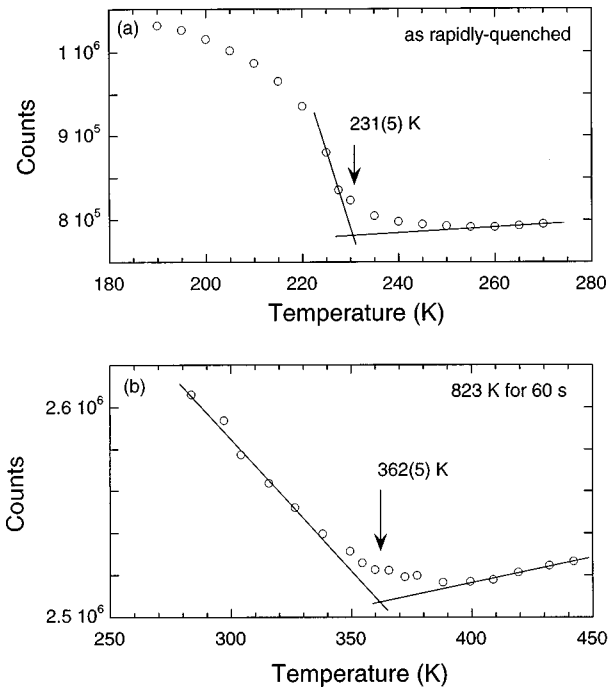

FIG. 5. Temperature dependence of the resonant γ-ray absorption at zero velocity for $Fe_{91}Zr_7B_2$ in a rapidly quenched state (a) and after annealing at 823 K for 60 s (b).

is suppressed to lower than the theoretical value for cubic anisotropy (0.83) in the temperature range below $\sim$200 K where small H_c values less than 10 A/m are obtained. This result is consistent with the plots in Fig. 1 where the samples with low H_c values generally reflect uniaxial anisotropy symmetry which indicates that the contribution of induced anisotropies to $\langle K\rangle$ may no longer be negligible (i.e., $\langle K\rangle \neq \langle K_1\rangle$) below $\sim$200 K.

V. DISCUSSION

A. Temperature dependence of coercivity

It is well known that H_c of materials generally depends on both the saturation magnetization (M_s) and the effective anisotropy constant $\langle K\rangle$ and can be expressed as

$$H_c = p_c \frac{\langle K\rangle}{M_s}, \tag{11}$$

where p_c is a constant; a value of $p_c \sim 0.2$ was estimated for nanocrystalline Fe-Si-B-Nb-Cu alloys[11] using $\langle K\rangle$ in Herzer's model ($\varphi = 1$). Given the fact that the fine particle theory for cubic crystals predicts $p_c = 0.64$, the assumed φ in

TABLE I. The mean ^{57}Fe hyperfine field at 0 K $\langle B_{\rm hf}(0)\rangle$, and the Curie temperature T_C derived from the fits shown in Fig. 4. The T_C values obtained from the Mössbauer thermal scan in Fig. 5 are also shown for comparison.

Sample	$\langle B_{\rm hf}(0)\rangle$ (T)	T_C (K)	T_C from thermal scan (K)
As rapidly quenched	21.3	228	231
823 K for 60 s	20.8	375	362

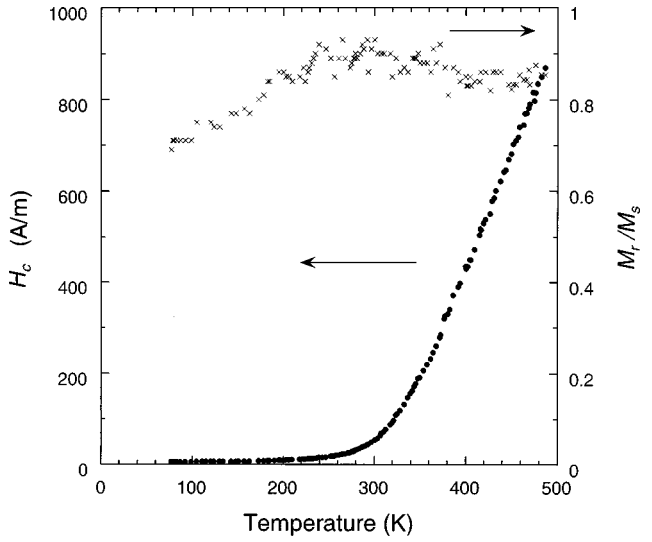

FIG. 6. Temperature dependence of the coercivity (H_c) and the remanence to saturation ratio (M_r/M_s) for nanocrystalline $Fe_{91}Zr_7B_2$ annealed at 823 K for 60 s.

Herzer's approach appears to be reasonable. Consequently, $H_c(T)$ for the present nanocrystalline Fe-Zr-B sample can be described by

$$H_c(T) \approx p_c(1-V_{\rm am})^2 \frac{K_1^4(T)D^6}{M_s(T)A^3(T)} \propto \frac{K_1^4(T)}{M_s(T)A^3(T)}. \tag{12}$$

Since H_c in the nanocrystalline Fe-Zr-B sample increases by two orders of magnitude towards $T_C^{\rm am}$ and H_c varies linearly with $1/M_s$, $M_s(T)$ cannot be responsible for such a dramatic increase in H_c. The H_c-T curve may also reflect $K_1(T)$ but K_1 of bcc-Fe decreases with temperature and thus $K_1(T)$ does not explain the observed positive temperature dependence of H_c in Fig. 6, indicating that $A(T)$ is indeed the dominant temperature-dependent factor for $H_c(T)$ in the present case.

In our nanocrystalline $Fe_{91}Zr_7B_2$ sample, the effective value of A is determined by the exchange stiffness in the bcc-amorphous-bcc coupling chain and thus the observed H_c-T curve in Fig. 6 should represent how the exchange coupling over the range of $L_{\rm ex}$ is determined in the two-phase nanocrystalline materials. A formulation of the effective A in two-phase nanocrystalline materials has been reported by Hernando *et al.*[10] They assumed that the decay of the Fe exchange field in the intergranular region is exponential and they introduced a phenomenological parameter γ. In this model, the effective exchange stiffness is given by substituting γA for A, where γ varies as

$$\gamma = e^{-\Lambda/L_{\rm am}}, \tag{13}$$

where $L_{\rm am}$ is the exchange correlation length in the amorphous matrix ($\sim\sqrt{A_{\rm am}/K_u^{\rm am}}$, where $A_{\rm am}$ and $K_u^{\rm am}$ are the exchange stiffness constant and the induced uniaxial anisotropy for the amorphous matrix phase, respectively.). Λ is the thickness of the residual intergranular amorphous phase. This model explained successfully the magnetic hardening at an early stage of the nanostructural evolution in the nanocrystalline soft magnetic materials by taking into account the magnetoelastic effect. In this approach, the temperature-dependent parameter which is relevant to the effective exchange stiffness is $L_{\rm am}$. Since $L_{\rm am}$ is expected to increase with temperature towards $T_C^{\rm am}$,[10] this model produces a positive temperature dependence for γ in the temperature range below $T_C^{\rm am}$ and thus cannot explain our experimental result shown in Fig. 6 in which H_c increases with T even below $T_C^{\rm am}$. In addition, the nanocrystalline $Fe_{91}Zr_7B_2$ sample clearly reflects the cubic anisotropy symmetry of K_1 and hence the uniaxial anisotropy $K_u^{\rm am}$ must be negligibly small in our case. Therefore, the increase in H_c in the nanocrystalline $Fe_{91}Zr_7B_2$ sample should be explained by other approaches. In the next section, we analyze the random magnetocrystalline anisotropy of the two-phase system incorporating two local exchange stiffness constants.

B. Two-phase random anisotropy model with two local exchange stiffness constants

In Herzer's two-phase random anisotropy model,[11] the angle between the nearest spin-spin pair within the coupled volume is assumed to be constant for both the nanocrystalline and intergranular regions (typically $d/\sqrt{A/\langle K\rangle}$ rad, where d is the spin-spin distance). However, if the exchange stiffness in the intergranular amorphous phase is lower than that of the crystalline phase the spin rotation should become more rapid within the amorphous part compared with that in the crystalline part with the higher exchange stiffness. We have considered two distinct angles for the spin-spin pairs in the crystalline and amorphous regions in order to include the effect of the exchange stiffness in the intergranular phase on the exchange correlation length. In our model, a simple cubic geometry has been assumed for the grains in order to maintain coherence with Herzer's original approach.

Our two-phase model starts from the same basic assumption in the original random anisotropy model[3] namely that the effective anisotropy constant ($\langle K\rangle$) which governs the anisotropy energy for the spin rotation over the exchange correlation length ($L_{\rm ex}$) is of the order of the square root of the mean-square fluctuation amplitude of the magnetocrystalline anisotropy energy within the magnetically coupled volume ($\sim L_{\rm ex}^3$). In a two-phase system where the exchange stiffness constants of the crystalline and amorphous phases are $A_{\rm cr}$ and $A_{\rm am}$, the spin rotation over each crystallite-amorphous coupling pair with the length $D+\Lambda$ would be

$$\varphi^0 = \frac{D}{\sqrt{A_{\rm cr}/\langle K\rangle}} + \frac{\Lambda}{\sqrt{A_{\rm am}/\langle K\rangle}} \tag{14}$$

with

$$\Lambda = D[(1-V_{\rm am})^{-1/3} - 1]. \tag{15}$$

Since the total spin rotation over the exchange correlation length is defined by φ, the number of grains within the entire coupling chain over $L_{\rm ex}$ is

$$n = \frac{\varphi}{\varphi^0} = \frac{\varphi}{D/\sqrt{A_{\rm cr}/\langle K\rangle} + \Lambda/\sqrt{A_{\rm am}/\langle K\rangle}}. \tag{16}$$

Furthermore, the magnetically coupled volume in this system is equal to

$$L_{\mathrm{ex}}^3=\frac{(nD)^3}{1-V_{\mathrm{am}}}, \tag{17}$$

and hence L_{ex} in the system is given by

$$L_{\mathrm{ex}}=\frac{1}{(1-V_{\mathrm{am}})^{1/3}}\frac{\varphi D}{\dfrac{D}{\sqrt{A_{\mathrm{cr}}/\langle K\rangle}}+\dfrac{\Lambda}{\sqrt{A_{\mathrm{am}}/\langle K\rangle}}}, \tag{18}$$

where $\langle K\rangle$ is given by

$$\langle K\rangle\approx\langle K_1\rangle=(1-V_{\mathrm{am}})\frac{K_1}{\sqrt{N}}, \tag{19}$$

and the total number of grains in the coupled volume N is

$$N=(1-V_{\mathrm{am}})\frac{L_{\mathrm{ex}}^3}{D^3}. \tag{20}$$

The exchange correlation length can be self-consistently determined using Eqs. (18)–(20) and one arrives at

$$L_{\mathrm{ex}}\approx\frac{1}{(1-V_{\mathrm{am}})^{7/3}}\frac{\varphi^4 D}{K_1^2(D/\sqrt{A_{\mathrm{cr}}}+\Lambda/\sqrt{A_{\mathrm{am}}})^4}, \tag{21}$$

and hence $\langle K\rangle$ in our new model is given by

$$\langle K\rangle\approx\frac{1}{\varphi^6}(1-V_{\mathrm{am}})^4K_1^4\left(\frac{D}{\sqrt{A_{\mathrm{cr}}}}+\frac{\Lambda}{\sqrt{A_{\mathrm{am}}}}\right)^6, \tag{22a}$$

or, equivalently,

$$\langle K\rangle\approx\frac{1}{\varphi^6}(1-V_{\mathrm{am}})^4K_1^4D^6\left[\frac{1}{\sqrt{A_{\mathrm{cr}}}}+\frac{(1-V_{\mathrm{am}})^{-1/3}-1}{\sqrt{A_{\mathrm{am}}}}\right]^6. \tag{22b}$$

It is worth noting that this final result of our model reproduces the same result of Herzer's two-phase model [Eq. (9)] under the condition $A_{\mathrm{cr}}=A_{\mathrm{am}}$ and for $V_{\mathrm{am}}=0$ our model reduces to the original single-phase nanocrystalline random anisotropy model [Eq. (5)]. Important features in the result of the above analysis are (i) the well-known D^6 dependence is preserved and (ii) $\langle K\rangle$ varies as A_{am}^{-3} under the condition $A_{\mathrm{am}}\ll A_{\mathrm{cr}}$, physically because the spin rotation within the exchange correlation length occurs mostly in the amorphous region. Some detailed simulations of $\langle K\rangle$ at various A_{am} and V_{am} values are given in Fig. 7. Furthermore, the calculated $\langle K\rangle$ curves have been normalized by the value at $A_{\mathrm{am}}=A_{\mathrm{cr}}$ (with the anisotropy $\langle K\rangle^*$) and replotted in Fig. 8. Constant parameters of $D=10$ nm, $K_1=10^4$ J/m^3, and $A_{\mathrm{cr}}=10^{-11}$ J/m^2, typical of Fe-based nanocrystalline soft magnetic alloys, were used in these $\langle K\rangle$ calculations.

The plots in Figs. 7 and 8 may explain some of the results in previous experimental work in two-phase nanocrystalline materials. It has commonly been observed[22,26] in previous studies for various two-phase nanocrystalline alloys that the increase in H_c near T_C^{am} becomes less prominent with the evolution of nanocrystallites in the sample (i.e., the decrease in V_{am}). Given the fact that the effect of A_{am} on the $\langle K\rangle$ value in Fig. 8 becomes more pronounced with increasing volume fraction of the residual amorphous phase, our model is fully consistent with these previously reported results. Figure 9 shows the effect of V_{am} on the calculated $\langle K\rangle$ at various A_{am} values. The $\langle K\rangle$ value for relatively low A_{am} exhibits a peak, predicting that H_c of the nanocrystalline alloys may increase at the initial stage of the nanocrystallite evolution. This prediction is only valid when the induced anisotropies of the amorphous precursor (K_u^{am}) is smaller than $\langle K_1\rangle$ and hence the $\langle K\rangle$ calculation in Fig. 9 does not seem to be relevant to the magnetic hardening in the Fe-Si-B-Nb-Cu

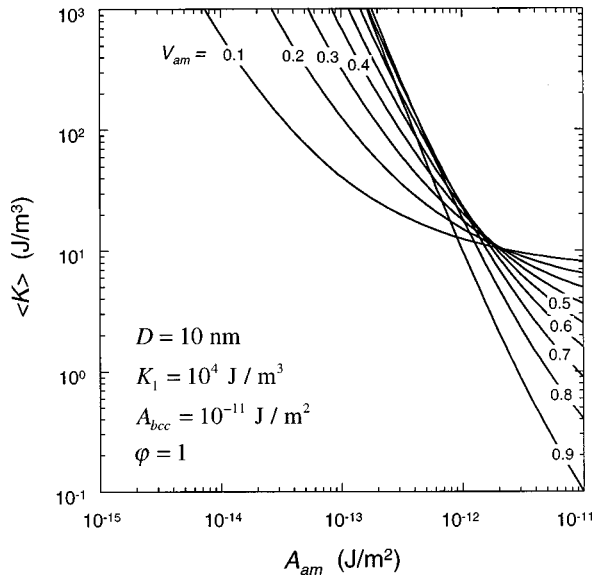

FIG. 7. Relation between the calculated $\langle K\rangle$ and the exchange stiffness constant of the residual amorphous phase (A_{am}) according to Eq. (22).

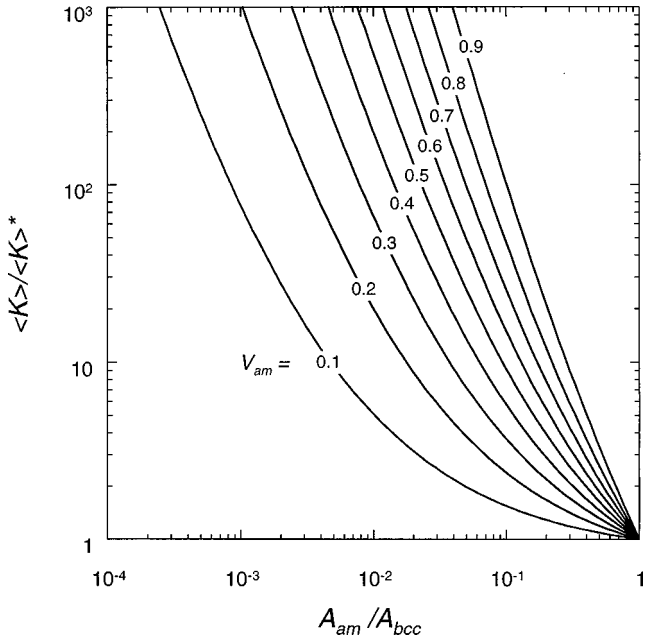

FIG. 8. Relation between the normalized random magnetocrystalline anisotropy ($\langle K\rangle/\langle K\rangle^*$) and the exchange stiffness constant ($A_{\mathrm{am}}/A_{\mathrm{cr}}$).

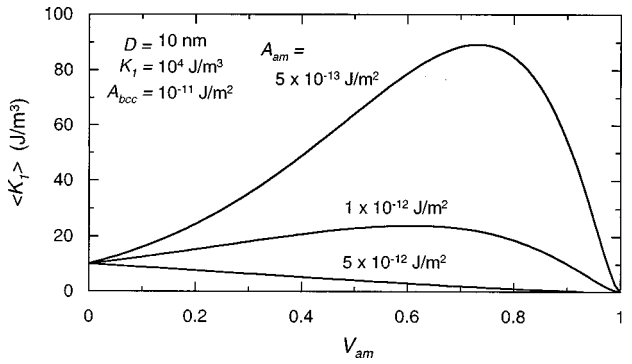

FIG. 9. Change in calculated $\langle K \rangle$ at various $A_{\rm am}$ as a function of the volume fraction of the residual amorphous phase ($V_{\rm am}$).

alloys for which a large $K_u^{\rm am}$ of ~ 100 J/m^3 and a small $\langle K_1 \rangle$ of ~ 2 J/m^3 were estimated.[11] However, the effect of $V_{\rm am}$ on the $\langle K \rangle$ value could be important in the Fe-Zr-B-Cu alloys where the H_c value in the amorphous state is comparable to that in the nanocrystalline state[27] (i.e., $K_u^{\rm am} \sim \langle K_1 \rangle$).

C. Application of the model to experimental results

In this section, we discuss the applicability of our model to actual two-phase nanocrystalline systems. The experimental results obtained from the nanocrystalline $Fe_{91}Zr_7B_2$ sample are explained based on the model proposed in the previous section.

It is known that the exchange stiffness constant of materials varies as

$$A \propto \frac{T_C S^2}{a}, \tag{23}$$

where S is the spin and a is the lattice parameter. Using the measured hyperfine fields at 295 K (12.4 T for the amorphous phase and 33 T for the crystalline phase), $T_C^{\rm am} \sim 370$ K and assuming that the Curie temperature of the bcc-Fe in the sample is ~ 1000 K, we obtain $A_{\rm am}/A_{\rm cr}$ of about 0.05 for the nanocrystalline $Fe_{91}Zr_7B_2$ alloy. Judging from the plot in Fig. 8, we find a considerably sharp variation of $\langle K \rangle$ at $A_{\rm am}/A_{\rm cr} \sim 0.05$ and $V_{\rm am} = 0.5$. Since $A_{\rm am}/A_{\rm cr}$ of the sample decreases dramatically towards $T_C^{\rm am}$, the observed increase in H_c towards $T_C^{\rm am}$ is well understood within the proposed model. More quantitative arguments are possible by looking at the relation between $H_c(T)$ and $\langle B_{\rm hf}(T) \rangle$. As we see in Fig. 10, the gradient of the ln H_c versus ln$\langle B_{\rm hf} \rangle$ plot tends to be steeper with decreasing $\langle B_{\rm hf} \rangle$ as is predicted in Fig. 8. In addition, the plot nearly matches the gradient of -6 at temperatures close to $T_C^{\rm am}$. This clearly indicates that $\langle K \rangle$ in the nanocrystalline $Fe_{91}Zr_7B_2$ sample is mostly governed by $A_{\rm am}^{-3}$ near $T_C^{\rm am}$, fully consistent with the above theoretical prediction.

Since the temperature dependence of H_c in the nanocrystalline $Fe_{91}Zr_7B_2$ alloy reflects $A_{\rm am}$ which varies as the square of the spontaneous magnetization, we should be able to obtain $T_C^{\rm am}$ from the H_c-T curve. The temperature dependence of the spontaneous magnetization for the residual amorphous phase ($M_s^{\rm am}$) near $T_C^{\rm am}$ is generally expressed by

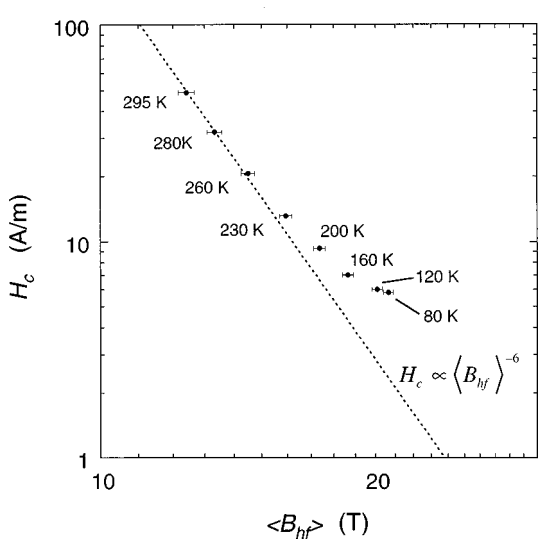

FIG. 10. Relation between ln H_c and ln$\langle B_{\rm hf} \rangle$ for the nanocrystalline $Fe_{91}Zr_7B_2$ alloy (replotted from Fig. 6).

$$M_s^{\rm am}(T) = M_0^{\rm am}\left(1 - \frac{T}{T_C^{\rm am}}\right), \tag{24}$$

where the critical exponent $\beta = 0.36$ has given reasonable fits to thermomagnetic curves in various nanocrystalline materials.[4,28] From this relation, one can expect that $A_{\rm am}(T)$ varies near $T_C^{\rm am}$ as $A_{\rm am}(T) \propto (T_C^{\rm am} - T)^{2\beta}$ and hence $\langle K(T) \rangle$ varies as

$$\langle K(T) \rangle \propto (T_C^{\rm am} - T)^{-6\beta}. \tag{25}$$

Using this relationship, a $T_C^{\rm am}$ value was estimated for the nanocrystalline $Fe_{91}Zr_7B_2$ alloy. The temperature dependence of H_c for the nanocrystalline $Fe_{91}Zr_7B_2$ alloy (Fig. 6)

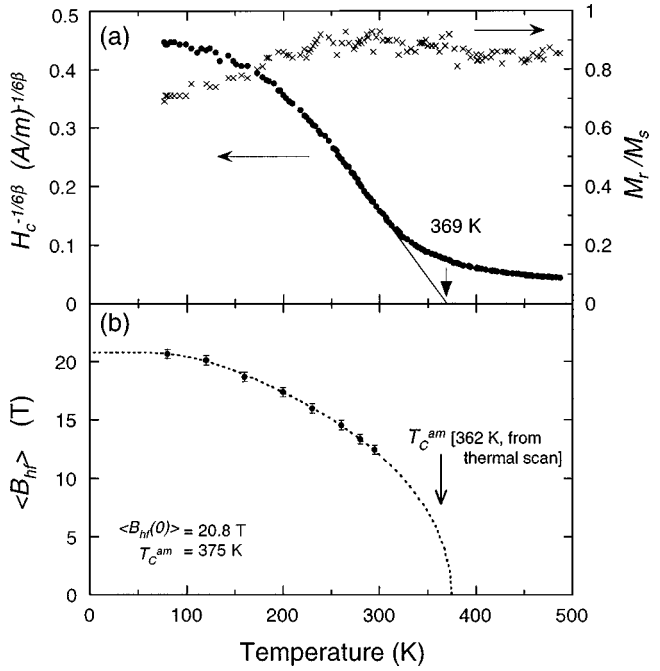

FIG. 11. Plots of the coercivity to the power $-1/6\beta$ ($\beta = 0.36$) (a) and the mean hyperfine-field (b) versus temperature for the nanocrystalline $Fe_{91}Zr_7B_2$ alloy.

is replotted as $H_c^{-1/6\beta}$ against T in Fig. 11(a). A critical temperature of 369 K is obtained by extrapolating the steepest straight part of the plots to the temperature axis. We have also estimated the effect of $K_1(T)$ and $M_s(T)$ on this critical temperature by assuming the relationship in Eq. (12) and using $K_1(T)$ of α-Fe (Ref. 29) and found that the obtained critical point in Fig. 11(a) could be overestimated by ~ 10 K. The obtained critical temperature is in good agreement with the Curie temperature shown in Fig. 11(b) where the $\langle B_{\rm hf}(T)\rangle$ results in Fig. 4 are replotted together with the fitting using the molecular field approximation. This agreement of the two critical temperatures reinforces our contention that the random magnetocrystalline anisotropy in the two-phase nanocrystalline systems can be well described by our extended model.

The critical point in Fig. 11 theoretically corresponds to the divergence of H_c (the maximum value is limited by K_1) due to the disappearance of the intergranular exchange coupling at $T_C^{\rm am}$, however, the experimental H_c in Fig. 6 keeps increasing even above this critical temperature. This clearly indicates that the contribution of magnetic interactions other than the direct ferromagnetic exchange interaction, such as the dipolar or the interaction due to the exchange penetration,[19] becomes significant near $T_C^{\rm am}$ (typically above $T/T_C^{\rm am}\sim 0.85$ in our case). These extra intergranular interactions limit the applicability of our two-phase random anisotropy model especially for those samples with small $V_{\rm am}$ since the effect of the exchange penetration is greater at short intergranular distances. Some other approaches[30] in which the exchange interactions over ferro-para-ferro-magnetic systems are considered could be useful in resolving the problem of the temperature dependence of H_c in the range very close to $T_C^{\rm am}$ or above.

VI. CONCLUSIONS

We have studied the effect of the exchange stiffness in the intergranular region on the random magnetocrystalline anisotropy ($\langle K_1\rangle$) both experimentally and theoretically. The temperature dependence of the coercivity (H_c) below the Curie temperature of the residual intergranular amorphous phase ($T_C^{\rm am}$) shows a clear correlation with the mean hyperfine-field of the residual amorphous phase ($\langle B_{\rm hf}\rangle$) derived from Mössbauer spectroscopy. The gradient of the $\ln H_c$ versus $\ln\langle B_{\rm hf}\rangle$ plot converges towards a value of -6 with increasing temperature towards $T_C^{\rm am}$, indicating that $\langle K_1\rangle$ in the sample varies as the -3rd power of the exchange stiffness constant of the residual amorphous phase ($A_{\rm am}$) near $T_C^{\rm am}$. The $A_{\rm am}^{-3}$ dependence has also been confirmed directly by the critical behavior in the H_c-T curve, $H_c \propto (T_C^{\rm am}-T)^{-6\beta}$, where $\beta\,(=0.36)$ is the critical exponent for the spontaneous magnetization.

These experimental results are quite well explained by the model proposed in the present study in which the two-phase random anisotropy model is extended by taking into account the effect of the two local exchange stiffness constants in the crystalline and amorphous regions on the exchange correlation length ($L_{\rm ex}$). We note that from our theoretical analysis (i) the well-known D^6 or K_1^4 dependences are preserved, (ii) the exponent for the $A_{\rm am}$ dependence of $\langle K\rangle$ converges towards a value of -3 for $A_{\rm am}\ll A_{\rm cr}$, where $A_{\rm cr}$ is the exchange stiffness constant of the crystalline phase, and (ii) the obtained formula [Eq. (22)] under the condition of $A_{\rm am}=A_{\rm cr}$ or $V_{\rm am}=0$ returns to the original results of Herzer.[5,11]

ACKNOWLEDGMENT

The authors are grateful to the Australian Research Council for its financial support.

*Author to whom correspondence should be addressed; Electronic address: suzuki@newt.phys.unsw.edu.au.

[1] See, for example, *Amorphous Metallic Alloys*, edited by F. E. Luborsky (Butterworth, London, 1983).
[2] Y. Yoshizawa, S. Oguma, and K. Yamauchi, J. Appl. Phys. **64**, 6044 (1988).
[3] R. Alben, J. J. Becker, and M. C. Chi, J. Appl. Phys. **49**, 1653 (1978).
[4] G. Herzer, IEEE Trans. Magn. **25**, 3327 (1989).
[5] G. Herzer, IEEE Trans. Magn. **26**, 1397 (1990).
[6] H. Q. Guo, T. Reininger, H. Kronmüller, M. Rapp, and V. K. Skumrev, Phys. Status Solidi A **127**, 519 (1991).
[7] M. Müller and N. Mattern, J. Magn. Magn. Mater. **136**, 79 (1994).
[8] K. Hono, Y. Zhang, A. Inoue, and T. Sakurai, Mater. Trans., JIM **36**, 909 (1995).
[9] M. Vázquez, P. Marin, H. A. Davies, and A. O. Olofinjana, Appl. Phys. Lett. **64**, 3184 (1994).
[10] A. Hernando, M. Vázquez, T. Kulik, and C. Prados, Phys. Rev. B **51**, 3581 (1995).
[11] G. Herzer, Scr. Metall. Mater. **33**, 1741 (1995).
[12] G. Le Caer and J. M. Dubois, Phys. Status Solidi A **64**, 275 (1981).
[13] E. C. Stoner and E. P. Wohlfarth, Philos. Trans. R. Soc. London, Ser. A **240**, 599 (1948).
[14] S. Chikazumi, *Physics of Magnetism* (Wiley, New York, 1964).
[15] K. Suzuki, A. Makino, A. Inoue, and T. Masumoto, J. Appl. Phys. **70**, 6232 (1991).
[16] K. Handrich, Phys. Status Solidi **32**, K55 (1969).
[17] J. M. Barandiarán, P. Gorria, I. Orúe, M. L. Fernández-Gubieda, F. Plazaola, J. C. Gómez Sal, L. Fernández Barquín, and L. Fournes, J. Phys.: Condens. Matter **9**, 5671 (1997).
[18] K. Suzuki, A. Makino, A. Inoue, and T. Masumoto, J. Appl. Phys. **74**, 3316 (1993).
[19] A. Hernando, I. Navarro, and P. Gorria, Phys. Rev. B **51**, 3281 (1995).
[20] S. N. Kaul, V. Siruguri, and G. Chandra, Phys. Rev. B **45**, 12 343 (1992).
[21] D. Kaptás, T. Kemény, L. F. Kiss, J. Balogh, L. Gránásy, and I. Vincze, Phys. Rev. B **46**, 6600 (1992).
[22] C. Gómez-Polo, D. Holzer, M. Multigner, E. Navarro, P. Agudo, A. Hernando, M. Vázquez, H. Sassik, and R. Grössinger, Phys. Rev. B **53**, 3392 (1996).
[23] M. Miglierini and J. M. Greneche, J. Phys.: Condens. Matter **9**, 2303 (1997).
[24] G. Le Caer, J. M. Dubois, H. Fischer, U. Gonser, and H. G. Wagner, Nucl. Instrum. Methods Phys. Res. B **5**, 25 (1984).
[25] H. Ren and D. H. Ryan, Phys. Rev. B **51**, 15 885 (1995).

[26] A. Hernando and T. Kulik, Phys. Rev. B **49**, 7064 (1994).
[27] K. Suzuki, M. Kikuchi, A. Makino, A. Inoue, and T. Masumoto, Mater. Trans., JIM **32**, 961 (1991).
[28] A. Ślawska-Waniewska, M. Gutowski, and H. K. Lachowicz, Phys. Rev. B **46**, 14 594 (1992).
[29] H. Gengnagel and U. Hofmann, Phys. Status Solidi **29**, 91 (1968).
[30] I. Navarro, M. Ortuno, and A. Hernando, Phys. Rev. B **53**, 11 656 (1996).